



EO4FLOOD

WATER CYCLE HYDROLOGY SCIENCE CLUSTER -
ADVANCING FLOOD FORECASTING

Requirement Baseline

ESA Contract 4000145540/24/I-EB

Project reference: EO4FLOOD_ESA_RB_D1.2
Issue:4.0
01/12/2025

Change Record

Date	Issue	Section	Page	Comment
29/10/2024	1.0			First version
15/05/2025	2.0	All	All	Second version
29/05/2025	3.0	1.2 2.7 2.8 3.4	5 19 24 30	Third version
01/12/2025	4.0	2.2 2.4 2.8	8-10 15-16 20-22	Fourth version

Control Document

Process	Name	Date
Written by:	A. Tarpanelli, L. Ciabatta, S. Barbeta, P. Filippucci, C. Massari, M.J. Tourian, P. Saemian, O. Elmi, C. Chewing, R. Palmitessa, P. Tamagnone, G. Schumann, D. Dettmering, D. Scherer, D. Gustafsson, Y. Hundecha, K. Nielsen, M. Sadki, V. Pedinotti, E. Cantoni, B. Revilla-Romero, K. Lernier	29/10/2024
Checked by	E. Volden, A. Vrettou	16/04/2025
Reviewed by	A. Tarpanelli, L. Ciabatta, S. Barbeta, P. Filippucci, C. Massari, M.J. Tourian, P. Saemian, O. Elmi, C. Chewing, R. Palmitessa, P. Tamagnone, G. Schumann, D. Dettmering, D. Scherer, D. Gustafsson, Y. Hundecha, K. Nielsen, M. Sadki, V. Pedinotti, E. Cantoni, B. Revilla-Romero, K. Lernier	15/05/2025
Checked by	E. Volden, A. Vrettou	28/05/2025
Reviewed	A. Tarpanelli	29/05/2025
Reviewed by	C. Massari, O. Elmi, A. Tarpanelli	01/12/2025
Approved by:		


	Signature	Date
For EO4FLOOD team	 Angelica Tarpanelli	01/12/2025
For ESA		

Table of Content

1. Introduction	5
1.1. Purpose and scope.....	5
1.2. Scope of the report	5
1.3. Applicable documents	5
1.4. Document Organization	5
2. Review of EO datasets and Methods	6
2.1. Precipitation	6
2.2. Soil Moisture	8
2.3. Snow	10
2.4. River width	15
2.5. Reflectance indices product	16
2.6. Multi-mission water level.....	17
2.7. Water surface slope.....	18
2.8. River discharge	19
2.9. Flood extent	24
3. Review of the rainfall-runoff and flood models	28
3.1. MGB rainfall-runoff model.....	28
3.2. DHI-GHM rainfall-runoff model	29
3.3. HYPE rainfall-runoff model.....	29
3.4. Hybrid AI model.....	30
3.5. MCP model	31
3.6. Mike+ model	32
3.7. HEC-RAS model	32
3.8. DassFlow1D/2D model	33
3.9. LISFLOOD-FP model.....	33
APPENDIX.....	35
Bramhaputra	35
Niger.....	36
Congo	38
Danube	39
Ebro.....	41
Negro	42
Po	43
Rhine.....	44
Torne.....	46

1. Introduction

1.1. Purpose and scope

The EO4FLOOD project aims at demonstrating the maturity and effectiveness of cutting-edge satellite data in enhancing flood forecasting systems. The project focuses on leveraging advanced satellite technologies and algorithms to improve the accuracy and timeliness of existing hydrological and hydraulic models, resulting in more reliable and precise flood predictions. EO4FLOOD is structured around three key pillars: 1) Development of an Advanced Open Earth Observation Dataset (EO4FLOOD dataset) that leverages the latest products from both ESA and non-ESA satellite missions, ensuring global coverage with high spatial and temporal resolutions; 2) Integration of the EO4FLOOD Dataset into Flood Forecasting Models through the combination of hydrological, hydraulic, and flood models with machine learning techniques; 3) Demonstration of the EO Data and Models for Science and Society to show how the integration of EO data and models can improve flood forecasting and risk management.

1.2. Scope of the report

This document is the Requirements Baseline for EO4FLOOD and represents D1.2 of the project. The document will review the status of products and processing algorithms, assessing their maturity and readiness for implementation before selecting them for use in generating the EO4FLOOD dataset. The document also outlines the dataset's content and coverage (both geographically and temporal), along with the source data and auxiliary information required for its production. The distinction between already existing methods and those newly introduced for the scope of the project is acknowledged, while the detailed description of all methodologies is provided in the deliverable *D2.2 Algorithm Theoretical Baseline Document (ATBD)*, to which this document refers. The document also specifies the EO products and in-situ data necessary to conduct the different validation activities.

1.3. Applicable documents

AD-01: Water Cycle Hydrology Science Cluster - Advancing Flood Forecasting – Statement of Work, V1.

1.4. Document Organization

After this introductory section, a review of the different input satellite and methods to derive them used within the EO4FLOOD project is found in Section 2, followed by the specification of the rainfall-runoff and flood models in Section 3. In Appendix, all the gauged stations identified in the study areas are listed. The EOdataset will be delivered in a subsample of such sites.

2. Review of EO datasets and Methods

This section describes the various EO products and methods to derive them used within the EO4FLOOD project. For every EO product the geographical extent, the temporal coverage, the maturity, the limitations and the latency are listed along with the reference.

2.1. Precipitation

Table 2.1.1: Information about the Precipitation product IMERG

Name	IMERG
Description	Integrated Multi-satellite Retrievals for GPM, based on the integration of passive microwave and infrared data through a constellation of satellites
Geographical extent	Global
Temporal coverage	2000-ongoing
Spatial resolution	0.1°
Temporal resolution	30 minutes
Data source	https://gpm.nasa.gov/data/directory
Maturity	Fully operational and available
Limitations	The quality is impacted by the number of microwave overpasses
Latency	The Early Run has a latency of about 4-6 hours, the Late Run of about 12-18 hours and the Final Run of about 3 months
Reference	Huffman, G. J., Bolvin, D. T., Nelkin, E. J., & Tan, J. (2015). Integrated Multi-satellite Retrievals for GPM (IMERG) technical documentation. Nasa/Gsfc Code, 612(47), 2019.

Table 2.1.2: Information about the Precipitation product CHIRPS

Name	CHIRPS
Description	Climate Hazards Group InfraRed Precipitation with Station data. The product is based on record precipitation estimates based on infrared Cold Cloud Duration (CCD) observations blended with stations data.
Geographical extent	50°S-50°N
Temporal coverage	Since 1981 to near present

Spatial resolution	0.05°
Temporal resolution	Daily
Data source	https://data.chc.ucsb.edu/products/CHIRPS-2.0/
Maturity	Fully operational and available
Limitations	3 weeks
Latency	Infrared data are expected to provide lower quality data
Reference	Funk, C., Peterson, P., Landsfeld, M. et al. The climate hazards infrared precipitation with stations—a new environmental record for monitoring extremes. <i>Sci Data</i> 2, 150066 (2015). https://doi.org/10.1038/sdata.2015.66

Table 2.1.3: Information about the Precipitation product SM2RAIN ASCAT

Name	SM2RAIN ASCAT
Description	Rainfall product based on the application of SM2RAIN algorithm to satellite soil moisture observations obtained through ASCAT data.
Geographical extent	Global
Temporal coverage	2007-2023
Spatial resolution	10 km
Temporal resolution	Daily
Data source	https://zenodo.org/records/6136294
Maturity	Operational through H SAF starting in Q2 2025
Limitations	The quality of the rainfall estimates is based on the reliability of the parent soil moisture products. Data with lower quality are expected over deserts, highly vegetated areas, regions characterized by high topographical complexity and frozen soils
Latency	Once operational, the product should be updated on a weekly basis
Reference	Brocca, L., Filippucci, P., Hahn, S., Ciabatta, L., Massari, C., Camici, S., Schüller, L., Bojkov, B., Wagner, W. (2019). SM2RAIN-ASCAT (2007-2018): global daily satellite rainfall from ASCAT soil moisture. <i>Earth System Science Data</i> , 11, 1583–1601, https://doi.org/10.5194/essd-11-1583-2019 .

Table 2.1.4: Information about the Precipitation product ERA-land

Name	ERA LAND
Description	ERA5-Land is a replay of the land component of the fifth generation ECMWF reanalysis (ERA5) for the global climate and weather. The dataset is produced without coupling with the atmospheric component.
Geographical extent	Global
Temporal coverage	1950-ongoing
Spatial resolution	0.1°
Temporal resolution	hourly
Data source	https://cds.climate.copernicus.eu/datasets/reanalysis-era5-land?tab=download
Maturity	Fully operational
Limitations	Model-based
Latency	5 days
Reference	Muñoz Sabater, J. (2019): ERA5-Land hourly data from 1950 to present. Copernicus Climate Change Service (C3S) Climate Data Store (CDS). https://10.24381/cds.e2161bac (Accessed on 20-OCT-2024)

2.2. Soil Moisture

Table 2.2.1: Information about the Soil Moisture product SMAP L3

Name	SMAP L3 Radiometer Global Daily 36 km EASE-Grid Soil Moisture, Version 6
Description	This L3 soil moisture product provides a composite of daily estimates of global land surface conditions retrieved by the SMAP radiometer. This product is a daily composite of SMAP L2 soil moisture which is derived from SMAP L1C interpolated brightness temperatures.
Geographical extent	Global
Temporal coverage	31/03/2015-ongoing
Spatial resolution	36 km
Temporal sampling	2–3 days (effective per grid cell), provided as a daily composite

Data source	https://n5eil01u.ecs.nsidc.org/SMAP/SPL3SMP.006/
Maturity	Fully operational, available at version 6, no follow-on missions
Limitations	Retrieval quality may be impacted by radio-frequency interference (RFI); radar instrument failed in 2015, so no active–passive retrievals available; performance may vary by vegetation density and surface conditions.
Latency	About 50 hours
Reference	O’Neill, P. E., et al. 2022. <i>SMAP L3 Radiometer Global Daily 36 km EASE-Grid Soil Moisture, Version 6</i> . NASA National Snow and Ice Data Center DAAC. https://doi.org/10.5067/W3DT1O4VMPB5

Table 2.2.2: Information about the Soil Moisture product SMOS L3 product.

Name	SMOS L3 (CATDS Level-3 Soil Moisture)
Description	The SMOS L3 soil moisture product provides daily global maps of surface soil moisture derived from MIRAS L-band brightness temperatures. The product applies temporal and spatial filtering to improve consistency and reduce noise, and is generated operationally by the Centre Aval de Traitement des Données SMOS (CATDS). Retrievals are based on the L-MEB model, which accounts for vegetation opacity, soil roughness, and soil dielectric properties.
Geographical extent	Global
Temporal coverage	January 2010 – ongoing
Spatial resolution	~36–50 km (depending on incidence angle and processing)
Temporal resolution	1–3 days (daily L3 product with effective sampling linked to SMOS multi-orbit coverage)
Data source	https://www.catds.fr/Products/Available-products-from-CEC-SM/CEC-SM-OS
Maturity	Fully operational; long-term climate data record
Limitations	Susceptible to radio-frequency interference (RFI); retrieval performance may degrade over dense vegetation or frozen soils
Latency	Typically 18 hours (depending on CATDS processing schedule)
Reference	Kerr, Y. H., et al. (2012). The SMOS mission: New tool for monitoring key elements of the global water cycle. <i>Proceedings of the IEEE</i> , 98(5), 666–687.

Table 2.2.3: Information about the Soil Moisture product H121, H101, H16, H104

Name	ASCAT L2 Surface Soil Moisture near-real time products H121
Description	Surface soil moisture estimates obtained through Metop-A, -B and -C platforms baskscatter. The product uses a change detection algorithm developed by TUWIEN.
Geographical extent	Global
Temporal coverage	2007-ongoing
Spatial resolution	12.5 km
Temporal resolution	Daily
Data source	https://hsaf.meteoam.it/
Maturity	Fully operational
Limitations	Quality impacted over deserts, deserts, highly vegetated areas, regions characterized by high topographical complexity and frozen soils.
Latency	1.5 hours
Reference	Wagner, W., Hahn, S., Kidd, R., Melzer, T., Bartalis, Z., Hasenauer, S., Figa-Saldaña, J., de Rosnay, P., Jann, A., Schneider, S., Komma, J., Kubu, G., Brugger, K., Aubrecht, C., Züger, J., Gangkofner, U., Kienberger, S., Brocca, L., Wang, Y., Blöschl, G., Eitzinger, J., Steinnocher, K., 2013. The ASCAT Soil Moisture Product: A Review of its Specifications, Validation Results, and Emerging Applications. Meteorologische Zeitschrift 5–33. https://doi.org/10.1127/0941-2948/2013/0399

2.3. Snow

Table 2.3.1: Information about the Snow cover product generated by the CLMS over Europe

Name	High Resolution Fractional Snow Cover (Copernicus Land – European component)
Description	Snow fraction as a percentage (0-100%) at the top of canopy and on ground, derived from the high-resolution optical satellite data acquired by Sentinel-2
Geographical extent	European
Temporal coverage	Sept. 2016 - present

Spatial resolution	20 m
Temporal resolution	5-day revisit
Data source	https://land.copernicus.eu/en/products/snow/fractional-snow-cover
Maturity	Fully operational. Major evolutions are currently being implemented by EEA (CLMS).
Limitations	Main limitations are related to the cloud coverage and solar illumination reduced in winter period. Challenge in snow detection in steep shaded slopes when the sun elevation is low. Uncertainty on the snow fraction estimated to +/- 25%.
Latency	Near real time (within 3 hours after the delivery of the Sentinel-2 L1C data)
Reference	<p>ATBD and PUM on the CLMS portal: https://land.copernicus.eu/en/products/snow/fractional-snow-cover</p> <p>Gascoin, S., Grizonnet, M., Bouchet, M., Salgues, G., and Hagolle, O. (2019) Theia Snow collection: high-resolution operational snow cover maps from Sentinel-2 and Landsat-8 data, Earth Syst. Sci. Data, 11, 493–514, https://doi.org/10.5194/essd-11-493-2019</p> <p>Let-It-Snow software, https://gitlab.orfeo-toolbox.org/remote_modules/let-it-snow, consulted on 15/01/2025</p>

Table 2.3.2: Information about the gap-filled Snow cover product generated by the CLMS over Europe

Name	High Resolution daily cumulative Gap-filled Fractional Snow Cover (Copernicus Land – European component)
Description	Snow fraction as a percentage (0-100%), derived from high resolution optical and radar satellite data acquired by Sentinel-2&1. Spatial gap-filling of S2 snow cover maps (FSC, Table 2.3.1) with S1 wet snow detection maps of the same day and temporal gap-filling with the aggregation of the past 7 days of observations.
Geographical extent	European
Temporal coverage	Sept. 2016 - present
Spatial resolution	60 m

Temporal resolution	1 day
Data source	https://land.copernicus.eu/en/products/snow/high-resolution-gap-filled-fractional-snow-cover
Maturity	Fully operational (CLMS)
Limitations	Added value of Sentinel-1 in mountainous areas only. While temporal aggregation increases the amount of usable information, it also assumes that a 7-day observation is still representative of current ground conditions.
Latency	Daily, with a latency of 3 hours maximum. The latency is defined as the time passed after the end of the day (23:59:59).
Reference	ATBD and PUM on the CLMS portal: https://land.copernicus.eu/en/products/snow/high-resolution-gap-filled-fractional-snow-cover

Table 2.3.3: Information about the Snow cover product generated by the CLMS over the Northern Hemisphere

Name	Snow Cover Extent (Copernicus Land – global component)
Description	Daily maps of the fraction of snow cover on ground (also in forested areas) per pixel in percentage (0% – 100%). Derived from the medium resolution optical satellite data from S-NPP VIIRS and S2 SLSTR.
Geographical extent	Northern Hemisphere (84°N/180°W to 25°N/180°E)
Temporal coverage	January 2018 - present
Spatial resolution	1 km
Temporal resolution	Daily
Data source	https://land.copernicus.eu/en/products/snow/snow-cover-extent-northern-hemisphere-v1-0-1km
Maturity	Fully operational
Limitations	Main limitations are related to the cloud coverage and solar illumination reduced in winter period. Misclassification of snow can occur in forested areas and in case of snow free ground but cold temperatures at night.
Latency	Within 1 day after the raw image acquisition

Reference	Metsämäki, S.; Mattila, O. - P.; Pulliainen, J.; Niemi, K.; Luojus, K.; Böttcher, K. (2012) An optical reflectance model-based method for fractional snow cover mapping applicable to continental scale. Remote Sensing of Environment, 123, 508 – 521. https://doi.org/10.1016/j.rse.2012.04.010
------------------	---

Table 2.3.4: Information about the snow dataset produced in the frame of the European Space Agency (ESA) Climate Change Initiative project

Name	ESA Snow Climate Change Initiative (Snow_cci) – climate research data package (CRDP)
Description	Snow Cover Fraction - Viewable snow (SCFV): snow viewable from space over all land surfaces, from optical imagery. In forested areas this refers to snow viewable on top of the forest canopy. Snow Water Equivalent (SWE), combining passive microwave data with ground-based snow depth measurements,
Geographical extent	SCFV : Global, excluding Antarctica and Greenland ice sheet and permanent snow and ice areas. The coastal zones of Greenland are included. SWE : Northern Hemisphere winter season (October – May; occasional data produced during June and September),
Temporal coverage	SCFV <ul style="list-style-type: none"> • Advanced Along-Track Scanning Radiometer (AATSR) – ENVISAT: May 2002- Apr. 2012 – v1.0 • Along-Track Scanning Radiometer 2 (ATSR-2) – ERS-2: v1,0 Aug, 1995 – June 2003 – v1.0 • Advanced Very High Resolution Radiometer (AVHRR) – POES & MetOp: Jan. 1979 – Dec. 2022 – v3.0 • Moderate resolution Imaging Spectroradiometer (MODIS) – Terra – Feb 2000 – Dec. 2022 – v3.0 SWE : Derived from SSMIS, SSM/I, SMMR, Nimbus 7 – Jan. 1979 – May 2022 – v3.1
Spatial resolution	SCFV AATSR/ ATSR-2 / MODIS: 1km SCFV AVHRR: 5km SWE: 0.1 degree
Temporal resolution	SCFV : Daily SWE : every second day from 1979 to May 1987, daily frequency starting in Oct. 1987.
Data source	https://catalogue.ceda.ac.uk/uuid/93cf539bc3004cc8b98006e69078d86b/

Maturity	Homogeneous, well calibrated, long-term time series. The project is scheduled for completion in February 2025.
Limitations	Revision and extension aligned with the CCI project delivery schedule.
Latency	In accordance with the CCI project delivery schedule.
Reference	Bibliography can be found online: https://catalogue.ceda.ac.uk/uuid/93cf539bc3004cc8b98006e69078d86b/

Table 2.3.5: Information about the Snow Water Equivalent product generated by the CLMS over the Northern hemisphere

Name	Snow Water Equivalent (SWE) (Copernicus Land – global component)
Description	Daily estimates of SWE, or the equivalent amount of liquid water stored in the snowpack, derived from a model assimilating both space-borne and in situ snow depth observations. SWE values are provided with a per pixel accuracy estimate.
Geographical extent	Northern Hemisphere (35°N-85°N)
Temporal coverage	2006 - present
Spatial resolution	5 km
Temporal resolution	Daily
Data source	https://land.copernicus.eu/en/products/snow/snow-water-equivalent-v1-0-5km
Maturity	Fully operational
Limitations	SWE is not estimated in mountain areas.
Latency	Within 12 hours since last input observation
Reference	<p>Pulliainen, J. Mapping of snow water equivalent and snow depth in boreal and sub-arctic zones by assimilating space-borne microwave radiometer data and ground-based observations. Remote Sensing of Environment 2006, 101, 257 – 269. https://doi.org/10.1016/j.rse.2006.01.002</p> <p>Takala, M.; Luojus, K.; Pulliainen, J.; Derksen, C.; Lemmetyinen, J.; Karna, J. - P.; Koskinen, J.; Bojkov, B. Estimating northern hemisphere snow water equivalent for climate research through assimilation of space-borne</p>

	<p>radiometer data and ground-based measurements. Remote Sensing of Environment 2011, 115, 3517 – 3529. https://doi.org/10.1016/j.rse.2011.08.014</p>
--	--

2.4. River width

Table 2.4: Information about the River width estimation

Name	Landsat 8-9, Sentinel-2
Description	<p>River width time series for the selected river reaches in this project are obtained from two sources: 1) satellite images from Landsat 8 and 9 with 30 m spatial resolution and 16 days revisit period are used to generate river width time series from 2014 2) Images from the Sentinel-2 missions (Sentinel-2A launched in 2015 and Sentinel-2B in 2017) are also employed to derive river width time series from 2015 onward. Sentinel-2 provides multispectral imagery at 10 m, 20 m, and 60 m spatial resolution, depending on the spectral band. The combined Sentinel-2A and 2B constellation provides a 5-day revisit period.</p> <p>To obtain the river width time series, we apply a modified version of the algorithm presented in Elmi & Tourian (2023). This method uses a region-based image segmentation approach to accurately extract river reach masks while maintaining both spatial and temporal consistency, resulting in a high-quality river width time series.</p>
Geographical extent	Global
Temporal coverage	Landsat 8: 2013-present, Landsat 9: 2022-present, Sentinel-2: 2015-present
Spatial resolution	Landsat 8-9: 30 m, Sentinel-2: 10, 20 m
Temporal resolution	Sentinel-2 has a temporal resolution of 5 days (with both satellites). Landsat 8 and Landsat 9 each have a 16-day revisit cycle, but together they provide an 8-day combined temporal resolution.
Data source	Google Earth Engine
Maturity	The algorithm has already been applied over numerous stations at global level. The code is written in Matlab and Python and freely accessible under request.
Limitations	Cloud coverage, relatively coarse spatial resolution for narrow rivers, relatively low temporal resolution
Latency	2-3 days

Reference	Elmi, O., & Tourian, M. J. (2023). Retrieving time series of river water extent from global inland water data sets. <i>Journal of Hydrology</i> , 617, 128880. https://doi.org/10.1016/j.jhydrol.2022.128880
------------------	---

2.5. Reflectance indices product

Table 2.5: Information about the Reflectance indices from MODIS and Sentinel-2

Name	Reflectance indices from MODIS and Sentinel-2
Description	<p>Reflectance indices, proxies for river discharge, are obtained for each selected river station using the data of MODIS and Sentinel-2. Reflectance indices are calculated from the Near-Infrared reflectance signal obtained from various environmental features in the river area (water, vegetation, periodically flooded areas, cities and roads), identified using the CM/CMW algorithm. Each satellite product is analyzed separately and then the obtained river discharge proxies are merged.</p> <p>The proxy time series are obtained using the Google Earth Engine Python API to analyze the MOD09GQ (MODIS TERRA), MYD09GQ (MODIS AQUA) and S2_HARMONIZED (Sentinel-2) collections. Reflectance data cannot be used to estimate river discharge on cloudy days, which are excluded from the analysis using appropriate masks. The temporal resolution of the proxy therefore depends on 1) satellite availability, 2) satellite overpass, 3) cloud masking.</p>
Geographical extent	global
Temporal coverage	2016-02-16 – to date
Spatial resolution	At the location of the selected gauges
Temporal resolution	3 - 5 days (average)
Data source	The product will be developed within the project
Maturity	The algorithm has already been applied over numerous stations at global level. The code is written in Matlab and Python and freely accessible under request.
Limitations	Cloud masking quality, cloud shadows, coarse resolution (MODIS), image coregistration (Sentinel-2)
Latency	3 days (in absence of clouds)
Reference	Filippucci, P., Brocca, L., Bonafoni, S., Saltalippi, C., Wagner, W., & Tarpanelli, A. (2022). Sentinel-2 high-resolution data for

	river discharge monitoring. Remote Sensing of Environment, 281, 113255. https://10.1016/j.rse.2022.113255
--	---

2.6. Multi-mission water level

Table 2.6.1: Information about the altimetry water level

Name	Database for Hydrological Time Series of Inland Waters (DAHITI)
Description	The DAHITI database provides water level time series of inland waters measured from satellite altimetry. Using nadir altimetry, the time series are available at the intersection (virtual station) of a satellite ground track with a river. DAHITI applies an extended outlier rejection and multi-mission cross-calibration. The accuracy of the water level time series varies between centimeters for large lakes and decimeters for small rivers.
Geographical extent	global
Temporal coverage	~2002 - ongoing (depending on available mission)
Spatial resolution	Virtual Stations
Temporal resolution	10 to 35 days (depending on available mission)
Data source	dahiti.dgfi.tum.de
Maturity	Well-Established public database
Limitations	The availability of DAHITI Virtual Stations is limited by the satellites' ground track, the sensor capabilities, and the river width and shape at the point of measurement.
Latency	NTC + STC (will be improved to NRT within this project)
Reference	Schwatke, C., Dettmering, D., Bosch, W., and Seitz, F. (2015) DAHITI – an innovative approach for estimating water level time series over inland waters using multi-mission satellite altimetry, Hydrol. Earth Syst. Sci., 19, 4345–4364, https://doi.org/10.5194/hess-19-4345-2015 .

Table 2.6.2: Information about the multi-mission water level

Name	Altimetry River Reach Methods (ARRM)
Description	Multi-mission-based water levels are derived via the R-packages ARRM (under development). Altimetry-based water levels from multiple missions located in space (along a river

	reach) and time are interpolated via a state-space model to achieve water level time series at a 2-10 km resolution along the reach
Geographical extent	Global
Temporal coverage	2010 - present
Spatial resolution	2-10 km along the considered reach
Temporal resolution	2-10 days (depending on available missions available on the reach)
Data source	The product will be developed within the project
Maturity	Mature, but not operational
Limitations	The method is limited by the amount and quality of available satellite altimetry missions
Latency	NTC can be updated with STC and NRT if available
Reference	Nielsen, K., Zakharova, E., Tarpanelli, A., Andersen, O.B. and Benveniste, J., 2022. River levels from multi mission altimetry, a statistical approach. Remote Sensing of Environment, 270, p.112876. https://doi.org/10.1016/j.rse.2021.112876

2.7. Water surface slope

Table 2.7.1: Information about the Water surface slope product

Name	Altimetry River Reach Methods (ARRM)
Description	Multi-mission-based surface slopes will be developed within the R-packages ARRM (under development). Altimetry-based water levels from multiple missions located in space (along a river reach) and time are interpolated via a state-space model to achieve water level time series at a 2-10 km resolution along the reach. The slope is then derived as the derivative of the water level.
Geographical extent	Global
Temporal coverage	2010-present
Spatial resolution	2-10 km
Temporal resolution	2-10 days
Data source	The product will be developed within the project

Maturity	Experimental. Details are provided in <i>D2.2_ATBD</i> document.
Limitations	The method is limited by the amount and quality of available satellite altimetry missions
Latency	NTC can be updated with STC and NRT if available
Reference	-

Table 2.7.2: Information about the ICESat-2 river surface slope product

Name	ICESat-2 river surface slope (IRIS)
Description	The global reach-scale “ICESat-2 River Surface Slope” (IRIS) dataset comprises average and extreme water surface slopes (WSS) derived from ICESat-2's synchronous lidar altimetry observations.
Geographical extent	Global
Temporal coverage	2018 - ongoing
Spatial resolution	10 km (reach-scale)
Temporal resolution	Average and extreme values between October 2018 and August 2024.
Data source	10.5281/zenodo.7098113
Maturity	Published dataset
Limitations	The number of observations is limited by cloud coverage. Only applied to reaches defined by SWORD.
Latency	3 to 6 months
Reference	Scherer D., Schwatke C., Dettmering D., Seitz F (2023): ICESat-2 river surface slope (IRIS): A global reach-scale water surface slope dataset. <i>Scientific Data</i> , 10(1), 359, https://10.1038/s41597-023-02215-x .

2.8. River discharge

Table 2.8.1: Information about the River discharge from width

Name	River discharge from river width
Description	The nonparametric quantile mapping algorithm (Elmi et al., 2021) will be applied to estimate river discharge from river

	width time series. This algorithm utilizes a stochastic quantile mapping scheme that iteratively generates realizations of river discharge and width time series through Monte Carlo simulation. It constructs a set of quantile mapping functions by matching all possible permutations of the simulated river discharge and width quantile functions. Measurement uncertainties are then adjusted based on the scatter of the point cloud. The algorithm iteratively updates the mapping function until convergence is achieved. Afterward, the river discharge estimates and associated uncertainties are derived from the river width measurements and the obtained mapping function.
Geographical extent	Global
Temporal coverage	Landsat 8: 2013-present, Landsat 9: 2022-present, Sentinel-2: 2015-present
Spatial resolution	10 km (reach-scale)
Temporal resolution	Depends on the satellite data availability can be varied from 5 to 16 days
Data source	Hydrosat.gis.uni-stuttgart.de
Maturity	Well-Established public database
Limitations	The gap in the data during cloud coverage.
Latency	Depends on satellite image latency
Reference	<p>Elmi, O., Tourian, M. J., Bárdossy, A., & Sneeuw, N. (2021). Spaceborne river discharge from a nonparametric stochastic quantile mapping function. <i>Water Resources Research</i>, 57(12), e2021WR030277. https://doi.org/10.1029/2021WR030277</p> <p>Tourian, M. J., Elmi, O., Shafaghi, Y., Behnia, S., Saemian, P., Schlesinger, R., & Sneeuw, N. (2022). HydroSat: geometric quantities of the global water cycle from geodetic satellites. <i>Earth System Science Data</i>, 14(5), 2463-2486. https://doi.org/10.5194/essd-14-2463-2022</p>

Table 2.8.2: Information about the river discharge from reflectance indices

Name	River discharge from multispectral indices
Description	The nonparametric quantile mapping algorithm (Elmi et al., 2021) will be applied to estimate river discharge from reflectance. This algorithm utilizes a stochastic quantile mapping scheme that iteratively generates realizations of river

	<p>discharge and reflectance time series through Monte Carlo simulation. It constructs a set of quantile mapping functions by matching all possible permutations of the simulated river discharge and reflectance quantile functions. Measurement uncertainties are then adjusted based on the scatter of the point cloud. The algorithm iteratively updates the mapping function until convergence is achieved. Afterward, the river discharge estimates and associated uncertainties are derived from the reflectance measurements and the obtained mapping function.</p>
Geographical extent	Global
Temporal coverage	2016/02/16 to date
Spatial resolution	At the location of the selected gauges
Temporal resolution	<5 days
Data source	The product will be developed within the project
Maturity	The algorithm has already been applied over numerous stations at global level. The code is written in Matlab and freely accessible under request.
Limitations	For completely ungauged river site the parameters of the regression laws cannot be calibrated, therefore their fixed values can induce not well accurate estimates of river discharge.
Latency	Depends on the latency of the satellite used for deriving the reflectance indices
Reference	<p>Tarpanelli A., Brocca L., Melone F., Moramarco T., Lacava T., Faruolo M., Pergola N., Tramutoli V. (2013) Toward the estimation of river discharge variations using MODIS data in ungauged basins. <i>Remote Sensing of Environment</i>, 136, 47–55. http://dx.doi.org/10.1016/j.rse.2013.04.010</p> <p>Tarpanelli A., Iodice F., Brocca L., Restano M., Benveniste J. (2020). River flow monitoring by Sentinel-3 OLCI and MODIS: comparison and combination. <i>Remote Sensing</i>, 12(23), 3867. https://doi.org/10.3390/rs12233867</p> <p>Tarpanelli A., Domeneghetti A. (2021) Flow duration curves from surface reflectance in the Near Infrared band. <i>Applied Sciences</i>, 11(8), 3458. https://doi.org/10.3390/app11083458</p>

Table 2.8.3: Information about the river discharge from water level

Name	River discharge from Water Level
Description	The nonparametric quantile mapping algorithm (Elmi et al., 2021) will be applied to estimate river discharge from water level time series. This algorithm utilizes a stochastic quantile mapping scheme that iteratively generates realizations of river discharge and water level time series through Monte Carlo simulation. It constructs a set of quantile mapping functions by matching all possible permutations of the simulated river discharge and water level quantile functions. Measurement uncertainties are then adjusted based on the scatter of the point cloud. The algorithm iteratively updates the mapping function until convergence is achieved. Afterward, the river discharge estimates and associated uncertainties are derived from the river water level measurements and the obtained mapping function.
Geographical extent	Global
Temporal coverage	From 2016 to date
Spatial resolution	At the location of the selected gauges
Temporal resolution	Between 10 and 27 days
Data source	Partially existent (see References), additional will be developed within the project
Maturity	Robust methodology applied in several basins and cases from small to large rivers.
Limitations	Need for non EO ancillary discharge data
Latency	Depends on WL latency (i.e. can be STC)
Reference	<p>Tourian, M. J., Sneeuw, N., & Bárdossy, A. (2013). A quantile function approach to discharge estimation from satellite altimetry (ENVISAT). <i>Water Resources Research</i>, 49(7), 4174-4186. https://doi.org/10.1002/wrcr.20348</p> <p>Elmi, O., Tourian, M. J., Bárdossy, A., & Sneeuw, N. (2021). Spaceborne river discharge from a nonparametric stochastic quantile mapping function. <i>Water Resources Research</i>, 57(12), e2021WR030277. https://doi.org/10.1029/2021WR030277</p>

Table 2.8.4: Information about the river discharge from satellite data for ungauged basins

Name	River discharge from satellite data for ungauged basins
Description	The algorithm combines various space-based sensors (radar and lidar altimetry, high-res optical imagery) to derive reach-scale river bathymetry and slopes (IRIS). The unknown roughness coefficient required for the Manning equation is optimized based on the principle of mass conservation requiring only loose bounds and minimal expert interaction. The results include realistic uncertainties based on the uncertainty of the input quantities.
Geographical extent	Global
Temporal coverage	~2002 - ongoing (depending on available altimetry mission)
Spatial resolution	10 km (reach scale) if covered by satellite altimetry
Temporal resolution	10 to 35 days (depending on available altimetry mission)
Data source	DAHITI, PlanetScope, ICESat-2 River Surface Slope (IRIS)
Maturity	Currently applied to 27 globally distributed river reaches. Can be transferred to other reaches.
Limitations	Cannot be applied to braided rivers. Limited by the availability of PlanetScope data (cost) and the location of DAHITI virtual stations.
Latency	Depending on satellite altimetry data
Reference	Scherer D., Schwatke C., Dettmering D., Seitz F. (2024) Monitoring river discharge from space: An optimization approach with uncertainty quantification for small ungauged rivers. Remote Sensing of Environment, 315, 114434, https://10.1016/j.rse.2024.114434

Table 2.8.5: Information about the river discharge from multi-sensor river discharge

Name	River discharge from multi-sensor
Description	The algorithm combines the river discharges obtained by the different sources to maximize the information available from the satellite variables.
Geographical extent	Global
Temporal coverage	2016/02/16 to date
Spatial resolution	At the location of the selected gauges

Temporal resolution	<5 days
Data source	The product will be developed within the project
Maturity	The approach is still at the experimental status. However, based on the attempts already carried out over several stations the combination of the Level-3 products (derived river discharges) is preferable to the direct combination of the individual variables. However, some other attempts will be carried out to find the proper solution. Details are provided in <i>D2.2_ATBD</i> document.
Limitations	Currently not setup to run automatically for a global dataset.
Latency	The latency depends on the satellite products included in the algorithm.
Reference	Tarpanelli A., Brocca L., Barbetta S., Faruolo M., Lacava T., Moramarco T. (2015) Coupling MODIS and radar altimetry data for discharge estimation in poorly gauged river basin. <i>IEEE Journal of Selected Topics in Applied Earth Observations and Remote Sensing</i> , 8(1), 141-148. http://dx.doi.org/10.1109/JSTARS.2014.2320582 .

2.9. Flood extent

Table 2.9.1: Information about the Flood extent

Name	Sentinel-1 Flood extent
Description	Identification of flooded areas based on Sentinel-1 SAR imagery. Two methods are available: (1) The deviation-based approach using both VV and VH channels. This method is suited for most situations and (2) a classification algorithm designed to detect water under canopy. This method is particularly suited in densely vegetated areas and wetlands. While the first method can be applied independently, the second is conceived as a complementary module of the first. For each AOI, the suitability of each method will be assessed taking into account local characteristics (e.g. topography, vegetation, land cover, etc.), image availability, and technical requirements. The decision to use one method, the other, or a combination of both will be made accordingly.
Geographical extent	Global
Temporal coverage	January 2017- Present
Spatial resolution	90 m
Temporal resolution	Depending on relative orbit and time period:

	<ul style="list-style-type: none"> • Maximum revisit of 3 days 2017-2021 (Both S-1 A+B were operational) • Approximately 12 days from 2021 onwards, after the malfunction of S-1 B. <p>Revisit time is expected to increase soon, when S-1 C calibration phase will finish and will become operational.</p> <p>Note: Some earlier images are available, but the frequency of acquisition is low and often irregular.</p>
Data source	Unprocessed data: ESA, processed images are obtained from Earth Engine data catalogued
Maturity	Mature
Limitations	<ul style="list-style-type: none"> • Dependent on threshold selection. • Some false positives can appear over cropping areas. • Difficulties capturing the flood maximum extent due to the Sentinel-1 frequency of acquisition. • Commission error over semi-arid and arid areas. • Possible artifacts around large water bodies.
Latency	2 days
Reference	Borlaf-Mena, I., Cantoni, È., Franco-Nieto, A., Toro-Bermejo, M., Revilla-Romero, B., Rodriguez Serrano, A., Loescher, L., Monsef Abboud, D., Domenech, C., and Albergel, C.: A Comparative Analysis of Flood Frequency Mapping Approaches for Climate-Resilience in South Sudan, EGU General Assembly 2024, Vienna, Austria, 14–19 Apr 2024, EGU24-18873, https://doi.org/10.5194/egusphere-egu24-18873 , 2024.

Table 2.9.2: Information about the Flood extent

Name	Sentinel-2 Flood extent
Description	FloodSENS-ML model using a UNet and Squeeze and Excitation Network (explanatory AI). Can map under partial cloud cover. During the project, flood mapping from FloodSENS will be done for each AOI
Geographical extent	Globally (same as S-2). FloodSENS mapping is AOI (Area of Interest) based
Temporal coverage	2016 - present
Spatial resolution	10 m
Temporal resolution	Same as S-2 (6 days)

Data source	S-2 bands, Copernicus DEM
Maturity	TRL 7
Limitations	<ul style="list-style-type: none"> • Complete cloud cover is an issue; • Latency is dependent on S-2 image availability; • Restricted (for now) to one optical satellite mission (S-2) Requires re-training if results are sub-optimal
Latency	1-2 hours (20 minutes inference processing time)
Reference	<p>FloodSENS ESA InCubed development (2020-2022: ESA Contract No. 4000134419/21/I-NS-bgh). RSS-Hydro IP</p> <p>B. Gaffinet, R. Hagensieker, L. Loi and G. Schumann, "Supervised Machine Learning for Flood Extent Detection with Optical Satellite Data," <i>IGARSS 2023 - 2023 IEEE International Geoscience and Remote Sensing Symposium</i>, Pasadena, CA, USA, 2023, pp. 2084-2087, https://10.1109/IGARSS52108.2023.10282274.</p>

Table 2.9.3: Information about the flood extent

Name	VIIRS 5-day flood product
Description	<p>The VIIRS 375-m Flood Product, is a near real-time product derived from daytime VIIRS sensors mounted on the Suomi-NPP and NOAA-21 satellites. The VIIRS Flood Map depicts the flood status at the time of the overpass, along with additional information on the weather and land conditions.</p> <p>The VIIRS 5-day composite flood product is preferred over the daily product to minimize the effect of cloud cover. These composites are created using a maximal water-fraction composition process, deriving the maximal flood extent for a given flood event. The global VIIRS Compositing Flood Products are routinely produced and include both the daily and 5-day composited flood products.</p> <p>In order to improve the granularity of the flood product, a downscaling process is applied to enhance the spatial resolution from 375m to 90m. This process leverages the concept of height above nearest drainage (HAND), calculated from a hydrologically conditioned Digital Elevation Model (DEM) at 90m resolution. For each VIIRS pixel (375 m), the corresponding HAND pixels (90 m) are ordered by HAND value, marking the ones with the smallest vertical distance to a river as flooded.</p>
Geographical extent	Global land between 60°S and 75°N

Temporal coverage	January 2012- Present
Spatial resolution	90m (Original 375 m, downscaled by GMV to 90m)
Temporal resolution	Daily, aggregated into 5-days composites
Data source	NOAA https://space.oscar.wmo.int/instruments/view/viirs
Maturity	Mature product (Base product accuracy 80% under clear-sky conditions)
Limitations	<ul style="list-style-type: none"> • 375m native resolution. • Water reference map: The current water reference map used for global flood mapping is from global water bodies of ESA CCI and MODIS global water mask (MOD44W Version 006). It might not reflect the new reservoirs and other hydraulic projects built after 2015, which may take some normal water as flooding water. • Agricultural-related flooding: Some flooding water shown in the VIIRS flood maps may not be any hazard-related flooding, but from agriculture-related activities such as rice paddy planting and aquaculture. Images are affected by cloud cover that may be partially retained in the 5-day product. • Low spatial detail even after the downscaling process. Downscaling of permanent water bodies is not possible (no water fraction data), retaining the original resolution.
Latency	Less than a day (prior to the required GMV's post-processing).
Reference	<p>Sanmei Li, Donglian Sun, Mitchell D. Goldberg, Bill Sjoberg, David Santek, Jay P. Hoffman, Mike DeWeese, Pedro Restrepo, Scott Lindsey, Eric Holloway, Automatic near real-time flood detection using Suomi-NPP/VIIRS data, Remote Sensing of Environment, Volume 204, 2018, Pages 672-689, ISSN 0034-4257, 10.1016/j.rse.2017.09.032</p> <p>More info: https://www.ssec.wisc.edu/flood-map-demo/ Quick guide: VIIRSFloodDetectionMapQuickGuide.pdf</p> <p>ATBD: https://www.star.nesdis.noaa.gov/jpss/documents/ATBD/ATBD_VIIRS_Flood_Mapping_v1.0.pdf</p>

3. Review of the rainfall-runoff and flood models

This section describes the various models used within the EO4FLOOD project. For every rainfall-runoff model and flood model, the required input parameters and auxiliary data are listed, and the maturity and limitations of the products/methods are presented. For every EO product and/or method, the required input parameters and auxiliary data are listed, and the maturity and limitations of the products/methods are presented.

3.1. MGB rainfall-runoff model

Table 3.1: Information about the MGB model

Name	MGB
Description	Semi-distributed physical based rainfall-runoff model. Requires climate variables (model is fit for local and/or global databases) for estimation of ET and rainfall. These variables are interpolated at elementary-division level (mini basins)
Required input parameters	DEM (for basin topography and discretization), soil information, land cover, climate (relative humidity, wind, temperature, pressure, insolation), rainfall. DEM preferred resolution is 30m (0.01°) but 90m is possible (0.03°). Rainfall datasets are 0.1° x daily, climate datasets are 0.1° x daily/monthly.
Required auxiliary data	Improving water balance with EO datasets (ET, flooded areas, soil moisture); In situ discharge for calibration
Maturity	Research model, with regional/continental operational set-ups
Limitations	Requires calibration by sub-basin
Reference	Siqueira, V. A., Paiva, R. C., Fleischmann, A. S., Fan, F. M., Ruhoff, A. L., Pontes, P. R., ... & Collischonn, W. (2018). Toward continental hydrologic–hydrodynamic modeling in South America. <i>Hydrology and Earth System Sciences</i> , 22(9), 4815-4842. https://doi.org/10.5194/hess-22-4815-2018 Pontes, P. R. M., Fan, F. M., Fleischmann, A. S., de Paiva, R. C. D., Buarque, D. C., Siqueira, V. A., ... & Collischonn, W. (2017). MGB-IPH model for hydrological and hydraulic simulation of large floodplain river systems coupled with open source GIS. <i>Environmental Modelling & Software</i> , 94, 1-20. https://10.1016/j.envsoft.2017.03.029

3.2. DHI-GHM rainfall-runoff model

Table 3.2: Information about the DHI-GHM model

Name	DHI-GHM
Description	Distributed, global model based on the NAM (Nedbør-Afstrømnings Model) conceptual rainfall-runoff model. The model is forced with global climatic data and parametrized using open-source data. The model runs on 0.1 x 0.1 degree grids.
Required input parameters	DEM, soil information, land cover (note that the model is already parametrized at global scale), climatic forcing (precipitation [hourly], temperature [daily], potential evapotranspiration [daily]). All input parameters are processed at 0.1 x 0.1 degree resolution.
Required auxiliary data	Optional: updated land cover or soil information
Maturity	Operational
Limitations	Water use beyond a coarse irrigation method is not included. For example, operation of reservoirs, is not included and can impact fine time resolution results (though it may not affect yearly aggregated results to the same extent)
Reference	Murray, A. M., Jørgensen, G. H., Godiksen, P. N., Anthonj, J., Madsen, H. (2023) DHI-GHM: Real-time and forecasted hydrology for the entire planet. Journal of Hydrology 620, 129431. https://doi.org/10.1016/j.jhydrol.2023.129431

3.3. HYPE rainfall-runoff model

Table 3.3: Information about the HYPE model

Name	Hydrological Predictions for the Environment (HYPE)
Description	A continuous and semi-distributed process-based hydrological model that simulates components of the catchment water cycle at a daily or hourly time step. Normally, model outputs are generated at the sub-basin outlet.
Required input parameters	DEM(<=90m), soil information, landuse/landcover (<= 300m), climate forcing (daily temperature and precipitation at 2.5-25 km resolution depending on application and data availability)

Required auxiliary data	River discharge for model calibration/data assimilation; optional, lake and river water levels, snow depth, snow water equivalent, soil moisture for model calibration/data assimilation
Maturity	Operational at national, regional and global scales
Limitations	Does not run at sub-hourly time steps
Reference	Lindström, G., Pers, C., Rosberg, J., Strömqvist, J. & Arheimer, B. (2010) Development and testing of the HYPE (Hydrological Predictions for the Environment) water quality model for different spatial scales. <i>Hydrol. Res.</i> 41(3–4), 295–319. https://10.2166/nh.2010.007

3.4. Hybrid AI model

Table 3.4: Information about the Hybrid AI model

Name	Hybrid AI model
Description	Hybrid AI and physics-based model based on the DHI-GHM model (see section 3.2), to be produced for the project. Hybrid hydrological models employ various techniques for embedding input features extracted from EO data (Kraft et al, 2022) and are proven to outperform both physics-based and purely data-driven model for extreme events (Acuña Espinoza et al, 2025). The exact formulation of the AI component will be defined in agreement with the findings in the aforementioned studies and targeting the limitations identified in the DHI-GHM model for the same AOI. The Hybrid AI model is intended as a more advanced and flexible approach to embed the EO data into the physics-based model compared to conventional calibration or data assimilation.
Required input parameters	The hybrid AI model will inherit most of the required input parameters of the DHI-GHM model. Some of them will be bypassed by adding a direct EO-to-parameter or EO-to-state AI component. Therefore, the relevant EO data will eventually replace the bypassed input in comparison with the original physics-based model. The detailed selection of inputs to be replaced is still to be defined.
Required auxiliary data	Available measurements of river discharge as target for training
Maturity	Experimental: the approach has been validated in previous studies but the exact implementation is still to be developed and tested in conjunction with the specific physics-based model and AOI. Details are provided in D2.2_ATBD document.

Limitations	Limited explainability of the model output; requires consistent data availability and quality.
Reference	<p>Kraft, B., Jung, M., Körner, M., Koirala, S., Reichstein, M. (2022). Towards hybrid modeling of the global hydrological cycle. <i>Hydrology and Earth System Sciences</i>, 26, 1579-1614. https://doi.org/10.5194/hess-26-1579-2022</p> <p>Acuña Espinoza, E., Loritz, R., Kratzert, F., Klotz, D., Gauch, M., Álvarez Chaves, M., & Ehret, U. (2025). Analyzing the generalization capabilities of a hybrid hydrological model for extrapolation to extreme events. <i>Hydrology and Earth System Sciences</i>, 29, 1277–1294, https://doi.org/10.5194/hess-29-1277-2025</p>

3.5. MCP model

Table 3.5: Information about the MCP model

Name	Model Conditional Processor, MCP
Description	Bayesian approach for estimating the flood predictive uncertainty (PU) defined as the probability density of a future outcome conditional on all the available information, usually provided by model forecasts.
Required input parameters	Forecasts provided by different models with the same lead times, observed time series of the forecasted quantity (river discharge, water level)
Required auxiliary data	Threshold discharge values for threshold overcome probability estimate
Maturity	Operational
Limitations	The time series of observed discharge should be long enough for calibration purposes. High flood events should be included.
Reference	<p>Barbetta, S., Coccia, G., Moramarco, T., Brocca, L., Todini, E., 2017. Improving the effectiveness of real-time flood forecasting through Predictive Uncertainty estimation: the multi-temporal approach. <i>J. Hydrol.</i> 51, 555–576. https://doi.org/10.1016/j.jhydrol.2017.06.030</p> <p>Barbetta, S., Sahoo, B., Bonaccorsi, B., Nanda, T., Chatterjee, C., Moramarco, T., Todini, E., 2023. Addressing the effective real-time forecasting inflows to dams through predicitive uncertainty estimate. <i>J. Hydrol.</i> 620, 129512. https://doi.org/10.1016/j.jhydrol.2023.129512</p>

3.6. Mike+ model

Table 3.6: Information about the Mike+ model

Name	MIKE+
Description	Fully hydrodynamic 1- and 2-dimensional depth-averaged model capable of predicting flow and water level in river networks and adjacent areas.
Required input parameters	DEM, river network alignment, discharge and water level boundary time series time series, river cross-section geometry, man made interventions such as weirs, culverts, pumps, and reservoirs including their operation. Spatial and temporal resolutions of input parameters are flexible, but in general the highest resolution DEM and a daily input timeseries resolution is preferred.
Required auxiliary data	Measured flows and water levels for calibration.
Maturity	Fully functional and tested/validated all around the globe
Limitations	Valid for subcritical incompressible fluids with hydrostatic pressure.
Reference	User manuals are available: https://manuals.mikepoweredbydhi.help/latest/MIKEPlus.htm

3.7. HEC-RAS model

Table 3.7: Information about the HEC-RAS model

Name	HEC-RAS
Description	Hydrodynamic model that allows the user to perform one-dimensional steady flow, one and two-dimensional unsteady flow calculations to predict flow propagation and hydraulic variables, such as water depth and velocity.
Required input parameters	DEM [$\leq 30\text{m}$], land cover [$\leq 10\text{m}$], soil map [$\leq 250\text{m}$], discharge/water level time series [$\leq \text{hourly}$] and terrain slope as boundary conditions, river network and cross-section geometry [$\leq 1 \text{ km}$] (if the 1D configuration is implemented), man-made interventions such as weirs, bridges, culverts, pumps, and reservoirs.
Required auxiliary data	Measured flows/water levels, flood extent for calibration. Optional: Precipitation Time Series

Maturity	Fully functional and continuously upgraded since 1993
Limitations	Steep Bed Slopes (>10%), Multi-Dimensional Flow, Complex Pipe Systems
Reference	HEC-RAS official website: https://www.hec.usace.army.mil/software/hec-ras/

3.8. DassFlow1D/2D model

Table 3.8: Information about the DassFlow 1D/2D model

Name	DassFlow
Description	Fully hydrodynamic multi-D (1D or 2D or both) depth averaged model capable of simulating discharge, velocities and water depths in rivers and floodplain. Model is fully derivable and implements Sensitivity Analysis and 4D-VAR data assimilation method based on the adjoint of the code. Also implements rainfall input processing and infiltration model
Required input parameters	Digital Elevation Model, hydrodynamic constraints (channel overbanks, levees, etc.), gridded rainfall timeseries (radar, satellite), river cross-sections geometry (1D version), Land Cover, Soil properties. Spatial resolution: 0.5m to 10m (preferred), 30m possible depending on the region. Temporal resolution: hourly
Required auxiliary data	Measured water levels or flows or velocity timeseries for calibration (hourly or less)
Maturity	Fully functional, HPC ready and tested on multiple test cases with various spatio-temporal scales and flow regimes (subcritical, supercritical, mixed)
Limitations	Only valid for flows where vertical effects can be neglected, turbulence is negligible and pressure is hydrostatic
Reference	https://dasshydro.github.io/

3.9. LISFLOOD-FP model

Table 3.9: Information about the LISFLOOD-FP model

Name	LISFLOOD-FP 8.x and previous versions
-------------	--

Description	<p><u>Prior to v. 8.x:</u> Research code model employing simplified formulation of shallow water equations, including acceleration (only omitting advection), developed for using low-res EO data sources (Copernicus DEM, etc.).</p> <p><u>v. 8.x:</u> new discontinuous Galerkin shallow-water solver for multi-core CPUs and GPUs (under an open GPL license)</p>
Required input parameters	<p>DEM [$\leq 30\text{m}$], River Network, River Width (Bankfull), Discharge Time-Series [$\leq \text{hourly}$]</p>
Required auxiliary data	<p>Optional: Evaporation Time Series, Precipitation Time Series, Friction Map (Manning's n)</p>
Maturity	<p>Fully functional and tested/validated all around the globe</p>
Limitations	<p>Limitations when flow becomes super-critical (different solvers can be triggered though using different LISFLOOD-FP versions)</p>
Reference	<p>J., Kesserwani, G., Neal, J., Bates, P., and Sharifian, M. K.: LISFLOOD-FP 8.0: the new discontinuous Galerkin shallow-water solver for multi-core CPUs and GPUs, <i>Geosci. Model Dev.</i>, 14, 3577–3602, https://doi.org/10.5194/gmd-14-3577-2021, 2021: https://gmd.copernicus.org/articles/14/3577/2021/</p> <p>Neal, J., G.Schumann, and P.Bates (2012), A subgrid channel model for simulating river hydraulics and floodplain inundation over large and data sparse areas, <i>Water Resour. Res.</i>, 48, W11506, doi:10.1029/2012WR012514: https://agupubs.onlinelibrary.wiley.com/doi/10.1029/2012WR012514</p>

APPENDIX

The Table includes the sites used within the project where the historical records of river discharge data are available. The in-situ discharge data for the sites reported below will be used to calibrate/validate the methodologies proposed in the framework of the project.

Bramhaputra

Gauge_ID	Lat	Lon	Mean Q [m ³ /s]	start	end
440_CHP	28.83333397	89.76667023	2.7	1956-6-3	1956-12-12
314_CHP	29.29999924	92.19999695	18.0	1971-4-21	1977-12-30
307_CHP	29.28333282	88.90000153	30.9	1980-1-1	1982-12-30
312_CHP	29.63333321	91.15000153	62.7	1955-7-6	1965-12-30
315_CHP	30	93.91666412	97.1	1969-12-5	1970-12-30
342_CHP	30.33333397	94.80000305	130.7	1965-1-1	1965-12-30
327_CHP	29.88333321	93.25	144.0	1978-5-29	1982-12-30
325_CHP	29.16666603	87.68333435	174.1	1980-1-1	1982-12-30
310_CHP	30.10000038	91.34999847	198.0	1966-1-1	1972-12-30
301_CHP	29.33333397	89.71666718	306.2	1956-2-1	1982-12-30
341_CHP	29.95000076	91.90000153	319.4	1961-1-1	1962-12-30
317_CHP	30.29999924	94.76667023	377.5	1967-1-1	1969-12-30
328_CHP	29.75	94.15000153	479.8	1978-7-1	1982-12-31
2651080_GRDC	25.75	89.5	961.5	1985-4-3	1992-3-30
339_CHP	29.28333282	91.16666412	968.8	1955-7-1	1956-6-9
305_CHP	29.46666718	94.56666565	1230.5	1955-6-2	1982-12-30
2651100_GRDC	25.18000031	89.66999817	23280.7	1985-4-3	1992-3-30
BWDB-FFWC Noonkhawa	25.9198	89.7700		1957-1-1	2024-12-31
BWDB-FFWC Chilmari	25.5681	89.6789		1957-1-1	2024-12-31
BWDB-FFWC Kurigram	25.8227	89.6647		1946-1-1	2024-12-31
BWDB-FFWC Kaunia	25.7888	89.4389		1945-1-1	2024-12-31

Niger

Gauge_ID	Lat	Lon	Mean Q [m ³ /s]	start	end
1234200_GRDC	12.47000027	2.420000076	0.9	1963-5-20	1988-4-29
1234500_GRDC	13.88000011	5.329999924	1.4	1976-1-1	1987-4-29
1837501_GRDC	12.49166679	8.268610954	2.4	1973-6-30	1973-10-15
1234190_GRDC	12.73999977	2.240000001	3.5	1962-8-7	1981-11-8
1234650_GRDC	13.67000008	6.769999981	5.0	1976-1-1	1979-12-30
1234180_GRDC	12.96000004	2.319999933	6.3	1962-8-9	1988-4-29
1134310_GRDC	12.02000046	-5.679999828	17.9	1806-1-1	2023-5-1
1234130_GRDC	13.73330021	1.616700053	26.6	1956-1-1	2002-11-28
1734450_GRDC	12.35000038	2.730000019	33.5	1961-3-1	1979-1-11
1434850_GRDC	10.63000011	-6.21999979	34.7	1976-1-1	1993-12-30
1134060_GRDC	11.13000011	-8.199999809	41.6	1971-5-1	1979-12-30
1634350_GRDC	9.180000305	-10.06000042	45.6	1957-7-5	1978-12-30
1134080_GRDC	10.80000019	-7.670000076	46.4	1971-11-1	1992-12-30
1426340_GRDC	8.109999657	-5.409999847	82.4	1979-1-1	1982-12-30
1134650_GRDC	15.81999969	-3.700000048	124.6	1954-6-8	1992-12-30
1634500_GRDC	10.38329983	-9.300000191	165.1	1938-5-1	2020-5-29
1134200_GRDC	12.52000046	-6.800000191	184.9	1953-5-10	1992-12-30
1634600_GRDC	11.36999989	-9.609999657	193.5	1954-5-20	1978-12-30
1634400_GRDC	10.64999962	-9.866700172	234.3	1923-8-1	2002-11-20
1634420_GRDC	10.60000038	-9.729999542	256.2	1947-5-3	1979-12-30
1634800_GRDC	10.63000011	-8.680000305	287.6	1954-6-1	1978-12-30
1134480_GRDC	14.02000046	-4.25	382.3	1952-1-1	1992-12-30
1134040_GRDC	11.97000027	-8.229999542	401.6	1954-3-18	1990-12-30
1134505_GRDC	14.52999973	-4.21999979	477.5	1806-1-1	2023-5-1
1134300_GRDC	13.2166996	-5.900000095	493.1	1922-5-1	2001-4-29
1134600_GRDC	15.39999962	-4.230000019	531.7	1987-1-1	1990-12-30
1134450_GRDC	13.38000011	-4.920000076	553.7	1951-7-21	1992-12-30
1234201_GRDC	12.58329964	2.616699934	633.1	1985-6-2	2002-7-29
1234090_GRDC	14.61670017	0.983299971	723.8	1975-1-1	2002-10-29
1134030_GRDC	11.68330002	-8.666700363	868.8	1967-9-1	2001-4-28
1234150_GRDC	13.52000046	2.089999914	905.7	1929-1-1	2020-6-14
1134460_GRDC	14.14999962	-4.980000019	919.6	1922-6-21	1992-12-30
1134900_GRDC	15.66670036	0.5	968.4	1950-10-19	2001-4-29
1834110_GRDC	11.38329983	4.133299828	989.9	1984-1-1	2002-11-28
1134700_GRDC	16.26670074	-3.383300066	995.2	1924-1-1	2003-12-30
1734500_GRDC	11.86670017	3.383300066	1042.4	1952-6-23	2000-9-21
1134850_GRDC	16.93000031	-0.579999983	1108.6	1954-6-1	1992-12-30
1134500_GRDC	14.52999973	-4.21999979	1123.3	1922-1-1	2001-4-29
1634650_GRDC	11.25	-9.170000076	1165.7	1952-5-8	1979-12-30
1134100_GRDC	12.86670017	-7.550000191	1374.4	1907-1-1	2006-1-30



EO4FLOOD

1134250_GRDC	13.7166996	-6.050000191	1379.9	1925-1-1	2001-4-29
1134400_GRDC	13.94999981	-5.369999886	1513.0	1953-1-1	1992-12-30
1835900_GRDC	8.199999809	9.733300209	1954.6	1970-1-1	2002-10-29
1834101_GRDC	7.800000191	6.766699791	5104.6	1970-1-1	2006-2-28
ABN-DGRE Kendaii	14.6103	0.9906		1975-1-1	2024-12-31
ABN-DGRE Niamey	13.5107	2.0999		1929-1-1	2024-12-31
ABN-DGRE Sirba	13.7319	1.5984		1956-1-1	2024-12-31

Congo

Gauge_ID	Lat	Lon	Mean Q [m ³ /s]	start	end
1447500_GRDC	-1.399999976	15.06999969	7.9	1978-1-1	1980-12-30
1749030_GRDC	4.883333206	18.03333282	30.5	1985-4-1	1988-3-30
1749080_GRDC	4.533333302	18.46666718	39.5	1985-4-1	1994-3-29
1447100_GRDC	-4.599999905	14.93000031	40.0	1978-1-1	1980-12-30
1749510_GRDC	4.733333111	22.68333244	72.0	1987-4-1	1994-3-30
1553100_GRDC	-8.699999809	30.62000084	79.0	1978-10-1	1981-9-29
1749600_GRDC	5.033333302	25.14999962	143.8	1986-4-1	1994-3-29
1547400_GRDC	-10.94999981	31.06999969	176.1	1972-1-5	2004-12-30
1749050_GRDC	3.666666746	18.29999924	210.7	1986-5-1	1994-3-30
1447300_GRDC	-2.910000086	15.64999962	416.0	1978-1-1	1980-12-30
1547310_GRDC	-11.96660042	28.75	515.1	1956-10-1	2005-11-29
1748500_GRDC	3.183333397	16.11666679	584.1	1985-4-1	1994-3-30
1749500_GRDC	4.716666698	22.81666756	713.5	1986-5-1	1994-3-30
1150201_GRDC	-4.333333015	20.58333206	2073.4	1932-1-1	1959-9-29
1147012_GRDC	-2.950000048	25.91666603	2271.2	1933-1-1	1959-12-30
1749100_GRDC	4.366666794	18.58333397	3764.4	1911-3-6	2016-12-30
1147011_GRDC	-0.349999994	25.45000076	6846.8	1932-1-1	1959-12-30
1150200_GRDC	-3.18333292	17.38333321	8278.4	1932-1-1	1959-12-30
1147013_GRDC	-4.136666775	15.33333302	39051.3	1932-1-1	1959-12-30
HYBAM/CRREB AC	-4.30	15.30		1950-1-1	2023-12-31
CRREBAC/HYB AM	1.62	16.07		1940-1-1	2020-12-31
CRREBAC/HYB AM	4.37	18.61		1950-1-1	2020-12-31
CRREBAC	0.51	25.19			

Danube

Gauge_ID	Lat	Lon	Mean Q [m ³ /s]	start	end
6144200_GRDC	48.39582062	21.75003052	109.8	1950-11-1	2017-12-30
6742451_GRDC	45.38499832	24.2994442	112.6	1967-1-1	2010-12-30
6342510_GRDC	48.40696716	10.88800907	113.0	1959-11-1	2019-12-30
6246611_GRDC	47.16439819	15.31890011	117.0	1987-1-1	2017-12-30
6444600_GRDC	47.83333206	22.68333244	127.2	1930-11-1	1995-12-30
6744500_GRDC	47.78722382	22.87694359	130.1	1938-1-1	2008-12-30
6546802_GRDC	46.37099838	15.99619961	142.2	1961-1-1	2019-12-30
6246600_GRDC	46.71060181	15.63560009	143.8	1968-1-1	2001-12-30
6142620_GRDC	48.16049957	17.88250923	144.3	1920-11-1	2017-12-30
6243030_GRDC	47.27610016	11.39690018	165.0	1951-1-1	2017-12-30
6545101_GRDC	46.12200165	15.09060001	166.0	1993-3-1	2019-12-30
6342925_GRDC	48.67375183	12.69368076	167.7	1925-11-1	2019-12-30
6744200_GRDC	46.16083145	21.32166672	185.8	1952-1-1	2008-12-30
6444090_GRDC	48.09999847	22.81666756	187.7	1937-11-1	1995-12-30
6242250_GRDC	48.03939819	14.42669964	204.9	1965-1-1	2017-12-30
6742700_GRDC	45.55586243	27.51222229	206.6	1953-1-1	2010-12-30
6545150_GRDC	45.06999969	16.37999916	208.1	1978-1-1	1990-12-30
6547500_GRDC	44.58000183	21.12000084	220.8	1992-1-1	2010-12-30
6343500_GRDC	48.15862656	12.83433533	258.5	1826-11-1	2019-12-30
6545050_GRDC	45.89319992	15.6097002	279.3	1956-1-1	2019-12-30
6546801_GRDC	46.37099838	15.99619961	299.5	1806-1-1	2023-5-1
6342500_GRDC	48.75400162	11.42199993	309.9	1923-11-1	2019-12-30
6343100_GRDC	48.05929947	12.23423862	354.2	1826-11-1	2019-12-30
6342920_GRDC	48.87975311	12.74722195	453.3	1925-11-1	2019-12-30
6444200_GRDC	47.18333435	20.20000076	454.4	1988-1-1	1995-12-30
6444310_GRDC	47.88333511	21.06666756	467.8	1988-1-1	1995-12-30
6342800_GRDC	48.6766243	13.11516094	634.5	1900-11-1	2019-12-30
6243850_GRDC	48.43610001	13.44169998	729.4	1951-1-1	2017-12-30
6544100_GRDC	45.93291855	20.08250046	830.1	1971-1-1	2010-12-30
6444100_GRDC	46.25	20.16666603	838.6	1930-11-1	1999-12-30
6342900_GRDC	48.58240128	13.50436115	1411.5	1900-11-1	2019-12-30
6545800_GRDC	44.98125076	19.61833382	1534.7	1992-1-1	2010-12-30
6242400_GRDC	48.4007988	15.58640003	1847.7	1931-1-1	1975-12-30
6242700_GRDC	48.14944458	16.9402771	1920.7	1977-1-1	2017-12-30
6442450_GRDC	47.72999954	18.32999992	2214.3	1947-11-1	1995-12-30
6442500_GRDC	47.77999878	18.95000076	2301.3	1930-11-1	1999-12-30
6442600_GRDC	46	18.67000008	2357.3	1930-11-1	1999-12-30
6542200_GRDC	45.52999878	19.07999992	2709.9	1971-1-1	2009-12-30
6742201_GRDC	44.81472015	21.37944412	5320.2	1991-1-1	2008-12-30
6842200_GRDC	44.15999985	22.81999969	5479.0	1992-1-1	1999-12-30



EO4FLOOD

6842400_GRDC	43.84000015	23.23999977	5486.0	1992-1-1	1999-12-30
6742200_GRDC	44.70000076	22.42000008	5602.6	1840-1-1	1990-12-30
6842700_GRDC	43.63000107	25.35000038	5794.4	1992-1-1	1999-12-30
6842900_GRDC	44.13000107	27.26000023	5961.2	1992-1-1	1999-12-30
6742500_GRDC	43.62722015	25.3544445	6017.4	1931-1-1	2010-12-30
6742900_GRDC	45.21666718	28.71665764	6526.7	1931-1-1	2010-12-30

Ebro

Gauge_ID	Lat	Lon	Mean Q [m ³ /s]	start	end
9257_AFD	42.28971863	0.192164868	0.6	1992-10-1	2018-9-29
9183_AFD	41.68178177	0.721319199	0.9	1965-10-1	1992-9-29
9229_AFD	41.90244675	-0.772220969	1.2	1983-10-5	2018-9-29
9188_AFD	42.78552246	-3.043390989	2.8	1980-10-22	2018-9-29
9018_AFD	42.58035278	-0.552953005	6.4	1931-1-1	2018-9-29
9281_AFD	42.58086777	-2.875944614	6.5	2004-3-29	2018-9-29
9193_AFD	41.62224579	0.196609005	12.1	1989-4-14	2018-9-29
6226430_GRDC	41.66878128	-0.841700017	12.5	1973-10-1	2017-9-29
9195_AFD	42.50115204	-0.116373084	13.5	1967-10-1	1975-12-30
9172_AFD	42.54455566	0.197250634	14.5	1965-10-1	2018-9-29
9258_AFD	42.42658615	0.389177769	16.9	1992-10-1	2018-9-29
6226230_GRDC	42.79985809	-3.394150019	17.4	1963-10-1	2017-9-29
9282_AFD	42.59334946	-0.88151443	18.4	2004-11-3	2018-9-29
9173_AFD	42.10229492	0.240090102	18.8	1965-10-1	1971-9-29
9123_AFD	42.40603256	-0.650136948	26.4	1949-10-1	2018-9-29
9101_AFD	42.6178093	-1.209695101	28.4	1913-1-1	2018-9-29
9128_AFD	42.12441635	0.308969617	30.0	1949-10-1	1972-9-29
9069_AFD	42.79267883	-1.78857708	41.1	1931-1-1	2018-9-29
9169_AFD	41.90867233	0.890749335	46.8	1965-10-1	1974-9-29
9004_AFD	42.31666183	-1.799910069	50.6	1913-1-1	2018-9-29
6226310_GRDC	42.34534836	-1.647609949	63.2	1913-1-1	2017-9-29
6226650_GRDC	41.52444839	0.346569985	74.5	1929-1-1	2017-9-29
6226600_GRDC	41.45288849	0.41971001	79.4	1925-10-12	2017-9-29
9149_AFD	42.48656845	-2.529067755	99.9	1954-10-1	1998-9-29
9120_AFD	42.41758728	-2.204149008	104.7	1948-10-1	2018-9-29
6226400_GRDC	41.65856934	-0.881060004	222.7	1913-1-1	2017-9-29
6226300_GRDC	42.18008041	-1.694740057	227.4	1929-1-1	2017-9-29
9002_AFD	42.1819458	-1.693395615	228.0	1929-1-1	2018-9-29
9162_AFD	42.02253723	-1.555212259	230.3	1963-1-1	1988-9-29
9112_AFD	41.33026123	-0.37367177	246.1	1945-10-1	1998-9-29
9263_AFD	41.39998245	-0.474785954	304.3	2011-1-31	2018-6-20
9210_AFD	41.24333572	0.434015453	339.0	1980-10-1	1985-9-29
9027_AFD	40.81405258	0.521063149	427.7	1913-1-1	2018-9-29
6226800_GRDC	40.8132782	0.520659983	428.2	1806-1-1	2023-5-1
9029_AFD	41.36148071	0.289913476	494.3	1916-10-20	1968-9-29

Negro

Gauge_ID	Lat	Lon	Mean Q [m ³ /s]	start	end
3618715_GRDC	4.196100235	-60.79389954	72.5	1806-1-1	2023-5-1
3618700_GRDC	5.03000021	-60.5	93.4	1970-10-1	2019-10-30
3618121_GRDC	0.249400005	-69.78500366	133.0	1806-1-1	2023-5-1
3618740_GRDC	1.75	-62.28329849	134.7	1984-6-12	2019-6-29
3618711_GRDC	4.167500019	-60.52809906	148.9	1806-1-1	2023-5-1
3618200_GRDC	0.517799973	-60.46609879	162.1	1806-1-1	2023-5-1
14428000_ANA	0.227500007	-63.98830032	196.0	2000-9-22	2019-9-29
14526000_ANA	3.381099939	-59.81110001	203.4	1984-7-6	2020-10-30
3618600_GRDC	-0.85860002	-60.52000046	217.4	1806-1-1	2023-5-1
14526500_ANA	3.854700089	-59.6875	219.9	2006-12-14	2020-10-30
14740000_ANA	1.129199982	-60.22359848	256.2	2005-9-23	2020-9-29
3618731_GRDC	2.731699944	-62.01720047	275.4	1984-4-29	2019-7-30
3618115_GRDC	1.33920002	-68.68579865	318.6	1982-8-1	2008-10-30
3618150_GRDC	0.884199977	-62.62189865	495.1	1806-1-1	2023-5-1
3618722_GRDC	3.549700022	-63.1692009	595.3	1984-5-3	2019-8-30
14325000_ANA	-0.344399989	-67.53579712	812.2	1999-12-26	2019-9-29
14500000_ANA	3.464400053	-60.90969849	1293.5	1975-10-1	2021-3-30
3618720_GRDC	3.207799911	-60.57109833	1454.9	1806-1-1	2023-5-1
3618110_GRDC	1.074399948	-67.59470367	1865.0	1806-1-1	2023-5-1
3618950_GRDC	0.476900011	-69.12809753	2468.6	1977-12-2	2020-1-30
3618500_GRDC	1.821400046	-61.12360001	2997.3	1806-1-1	2023-5-1
3218050_GRDC	1.929999948	-67.12000275	4455.4	1978-1-1	1988-12-30
3618052_GRDC	-0.200599998	-66.80220032	12824.3	1806-1-1	2023-5-1
14420000_ANA	-0.481900007	-64.8289032	17642.4	1977-8-10	2020-1-30
3618051_GRDC	-0.481700003	-64.82720184	17642.4	1977-8-10	2020-1-30

Po

Gauge_ID	Lat	Lon	Mean Q [m ³ /s]	start	end
6948520_GRDC	46.20159912	9.168899536	0.5	1966-1-1	2018-12-31
6948111_GRDC	46.39899826	10.06719971	0.5	1970-1-1	2018-12-31
6948530_GRDC	46.22480011	8.015399933	0.8	1952-1-1	2018-12-31
6948360_GRDC	46.36959839	8.542900085	1.4	1967-1-1	2018-12-31
6948150_GRDC	46.01750183	8.962499619	2.5	1962-6-1	2018-12-31
6348202_GRDC	44.11999893	7.869999886	4.5	1936-1-1	2008-12-30
6948110_GRDC	46.29539871	10.07999992	5.9	1931-1-1	2018-12-31
6348310_GRDC	45.83000183	8.260000229	7.1	1936-1-1	2008-12-30
6948120_GRDC	46.16830063	8.773599625	23.1	1970-1-1	2018-12-31
6348201_GRDC	44.50999832	7.900000095	37.0	1942-1-1	2008-12-30
6948100_GRDC	46.19380188	9.009300232	68.7	1911-1-1	2018-12-31
6348300_GRDC	45.54990005	7.828100204	93.8	1936-1-1	2008-12-30
6348200_GRDC	44.94850159	8.685700417	127.7	1936-1-1	2008-12-30
6348600_GRDC	45.78340149	9.435899734	160.1	1946-1-1	2002-12-30
6348610_GRDC	45.84799957	9.392999649	165.3	1845-1-1	2016-12-30
6348350_GRDC	45.70100021	8.650699615	293.8	1923-1-1	1994-12-30
6348400_GRDC	45.01666641	9.666666985	928.6	1980-1-1	1985-12-30
6348500_GRDC	44.90000153	10.55000019	1233.9	1980-1-1	1985-12-30
6348800_GRDC	44.88333511	11.60000038	1538.7	1980-1-1	1985-12-30
Arpa_Piemonte	44.9086	7.6909	53.3	2016-1-1	2023-12-31
Arpa_Piemonte	45.1389	8.4361	143.5	2016-1-1	2023-12-31
Arpae	45.1018	9.3461	596.8	2016-1-1	2022-12-31
Arpae	45.0605	9.7055	763.6	2016-1-1	2024-12-31
Arpae	45.1283	9.9948	968.6	2016-1-1	2024-12-31
Arpae	45.0456	10.7591	1189.5	2016-1-1	2024-12-31
Arpae	44.8440	10.4540	8.7	2016-1-1	2022-12-31
Arpae	44.6349	10.1714	2.3	2016-1-1	2022-12-31
Arpae	44.8067	10.3251	7.4	2016-1-1	2022-12-31
Arpae	44.7272	11.0451	15.3	2016-1-1	2022-12-31
Arpae	45.5482	7.8248	89.1	2016-1-1	2022-12-31
Arpae	44.7475	10.9873	18.3	2016-1-1	2022-12-31
Arpae	44.5100	9.8400	14.1	2016-1-1	2024-12-31
Arpae	44.9169	10.2543	26.7	2016-1-1	2022-12-31
Arpa_Piemonte	44.5200	7.9000	30.0	2016-1-1	2022-12-31
Arpa_Piemonte	44.7056	8.0270	48.8	2016-1-1	2022-12-31
Arpa_Piemonte	45.3815	8.3740	24.4	2016-1-1	2023-12-31
Arpae	44.6327	9.4054	3.7	2016-1-1	2022-12-31
Arpae	44.6402	9.3300	4.1	2016-1-1	2022-12-31

Rhine

Gauge_ID	Lat	Lon	Mean Q [m ³ /s]	start	end
6935370_GRDC	46.96900177	7.192599773	0.6	1956-1-1	2007-12-30
6935150_GRDC	46.75669861	8.980500221	0.7	1963-1-1	1989-12-30
6935380_GRDC	46.54700089	7.757400036	1.4	1950-1-1	1982-12-30
6935120_GRDC	46.77679825	6.724199772	1.6	1971-1-1	2018-12-31
6935580_GRDC	46.81129837	8.598999977	1.6	1960-1-14	2018-12-31
6135110_GRDC	48.90270615	8.047980309	1.7	1965-1-1	2012-6-4
6935080_GRDC	46.8852005	7.501699924	2.6	1922-2-25	2018-12-31
6935065_GRDC	47.19680023	7.172200203	4.2	1961-1-1	2018-12-31
6335695_GRDC	48.71258163	9.418433189	9.7	1961-1-1	2019-12-30
6935314_GRDC	47.06961823	8.278424263	15.0	1936-1-1	2018-12-31
6336920_GRDC	49.13478851	7.181268215	18.8	1956-11-1	2018-12-30
6335450_GRDC	47.62799072	9.595916748	19.5	1932-1-1	2019-12-30
6335116_GRDC	49.77997971	7.720316887	25.7	1951-11-1	2018-12-30
6335031_GRDC	51.43598557	7.581097126	28.2	1950-10-30	2017-4-29
6335113_GRDC	49.94398499	7.898139954	29.0	2002-10-15	2019-3-30
6935401_GRDC	47.50579834	9.211600304	38.0	1965-1-1	2018-12-31
6335083_GRDC	51.74528503	7.186914921	38.0	1950-10-1	2019-6-24
6136200_GRDC	48.16461563	6.452055931	38.1	1960-1-1	2012-5-30
6335045_GRDC	50.79790115	7.159167767	51.2	1964-10-26	2019-10-23
6335530_GRDC	49.83419037	10.94127464	53.7	1922-11-1	2019-12-30
6336900_GRDC	49.40892792	6.648421764	72.2	1952-7-1	2019-12-30
6335601_GRDC	49.07339859	9.145666122	85.0	1948-11-1	2019-12-30
6335301_GRDC	50.03119659	10.2208147	103.1	1844-11-1	2018-12-30
6335500_GRDC	49.79600143	9.925999641	108.8	1823-11-1	2016-12-30
6935145_GRDC	46.83769989	9.456100464	117.2	1899-1-1	2018-12-31
6335600_GRDC	49.43824768	9.005031586	134.7	1950-11-1	2019-12-30
6935310_GRDC	47.42100143	8.271300316	139.0	1904-1-1	2018-12-31
6335302_GRDC	50.00999451	9.60386467	142.0	1964-11-1	2018-3-31
6336800_GRDC	49.47257614	6.369034767	150.0	1974-11-1	2019-12-30
6235535_GRDC	47.27444458	9.534999847	151.5	1996-1-1	2017-12-30
6335240_GRDC	49.71647644	9.224583626	163.2	1958-11-1	2019-12-30
6335304_GRDC	50.10577393	8.714985847	185.4	1963-11-1	2019-12-30
6336500_GRDC	49.73218918	6.626852989	277.5	1930-11-1	2019-12-30
6935302_GRDC	47.26660156	7.830599785	285.1	1916-1-1	2018-12-31
6336050_GRDC	50.14335251	7.168275833	312.3	1900-11-1	2019-12-30
6935055_GRDC	47.68230057	8.625900269	368.7	1904-1-1	2018-12-31
6935054_GRDC	47.57040024	8.329999924	440.4	1904-1-1	2018-12-31
6935052_GRDC	47.55989838	7.588399887	1042.4	1869-1-1	1995-12-30
6335170_GRDC	49.32380676	8.448717117	1269.2	1950-11-1	2020-3-30
6335180_GRDC	49.64112091	8.376018524	1409.7	1930-1-1	2020-3-30



EO4FLOOD

6335150_GRDC	50.00398636	8.275313377	1672.8	1981-1-1	2018-10-30
6335070_GRDC	50.44338608	7.392049789	2034.3	1930-11-1	2018-10-31
6335050_GRDC	51.22554779	6.770183086	2119.5	1900-11-1	2019-12-30
6335020_GRDC	51.75691986	6.395394802	2246.2	1814-11-1	2019-12-30

Torne

Gauge_ID	Lat	Lon	Mean Q [m ³ /s]	start	end
6832754_GRDC	68.74810028	21.41588783	0.1	1975-7-12	2019-1-28
6832909_GRDC	68.88047028	21.07643318	1.6	1959-5-1	2015-12-30
6832929_GRDC	66.82673645	24.38655472	4.1	1985-1-1	2013-12-30
6832753_GRDC	68.93840027	20.85219955	4.9	1952-9-6	2013-12-30
6232916_GRDC	68.36000061	18.78000069	14.4	1985-4-9	2018-6-22
6832752_GRDC	66.3813324	23.78398323	31.1	1959-1-1	2017-12-30
6232930_GRDC	68.02999878	21.97999954	46.8	1923-1-1	2018-5-13
6232100_GRDC	68.36000061	18.80999947	62.9	1918-1-1	1998-12-30
6232101_GRDC SMHI	68.34999847	18.81999969	63.5	1918-1-1	2019-1-17
6232915_GRDC	67.43000031	22.51000023	68.3	1967-8-15	2018-7-2
6232905_GRDC	68.43000031	22.47999954	85.1	1972-1-1	2017-12-31
6832907_GRDC SMHI/SYKE	68.44228363	22.49458122	85.2	1972-1-1	2017-12-30
6832750_GRDC SYKE	67.9457016	23.66010094	125.0	1938-1-1	2017-12-30
6232913_GRDC	67.43000031	22.45000076	132.2	1967-8-15	1975-5-9
6232900_GRDC	67.22000122	23.54999924	159.5	1911-1-1	1988-12-30
6232901_GRDC	67.22000122	23.54000092	165.5	1911-1-2	2018-7-6
6832917_GRDC	66.78524017	23.91239929	343.8	1959-1-1	2013-12-30
6232910_GRDC	65.97000122	24.04999924	388.2	1911-1-1	2017-12-31
SYKE	66.144	23.9251			
SYKE	66.7768	23.9684			
SMHI	68.046	21.9878			